DOI: 10.1002/zaac.200500502

The Iron Hydrido Complex $[FeH(dppe)_2]^+$: Solution and Solid-State Reactivity with Dinitrogen

Oliver Franke[a], Beatrix E. Wiesler[b], Nicolai Lehnert[a], Gerhard Peters[a], Peter Burger[c], and Felix Tuczek[a,*]

[a] Kiel, Institut für Anorganische Chemie, Christian-Albrechts-Universität
[b] Mainz, Institut für Anorganische und Analytische Chemie, Johannes Gutenberg Universität
[c] Hamburg, Institut für Anorganische Chemie, Universität

Received December 19th, 2005.

Dedicated to Professor Hanskarl Müller-Buschbaum on the Occasion of his 75th Birthday

Abstract. The blue compound $[FeH(dppe)_2]BPh_4$ (**1**) (dppe = 1,2-bis(diphenylphosphino)ethane) is investigated by optical absorption, vibrational, NMR and Mössbauer spectroscopy as well as magnetic susceptibility measurements. In the solid state, **1** is found to be paramagnetic (S=1) whereas in tetrahydrofuran (thf) solution it is diamagnetic. Importantly, **1** reacts with dinitrogen in thf solution and in the solid state to give the yellow and green dinitrogen complexes **2a** and **2b**, respectively, both of which have the formula $[FeH(N_2)(dppe)_2]BPh_4$. Apart from their colour and optical spectroscopic properties, the dinitrogen compounds **2a** and **2b** also differ in their magnetic, Mössbauer and vibrational properties. The N-N stretching frequency of **2a** is found at $2120\ cm^{-1}$ whereas **2b** exhibits an N-N stretching vibration of $2145\ cm^{-1}$. Moreover, **2a** is diamagnetic whereas **2b** is paramagnetic. DFT is employed to determine the relative energies and structure of **1** and its dinitrogen adducts in the singlet and triplet state.

Keywords: Nitrogen fixation; Iron; Infrared spectroscopy; Mössbauer spectroscopy; NMR spectroscopy

Introduction

In spite of the dominant role of iron in the enzyme nitrogenase and in the catalyst of the Haber-Bosch process, low molecular weight mono- and dinuclear iron-dinitrogen complexes exhibit only a limited activity with respect to the transition-metal mediated generation of ammonia from N_2 [1]. The reason for this situation lies in the fact that most of the characterized Fe-N_2 complexes have divalent iron atoms which do not activate dinitrogen towards protonation [2]. Low-valent iron complexes (Fe^I, Fe^0) are *a priori* more effective in reproducing this ability of the enzymatic system. Accordingly the generation of NH_3 has been achieved with an Fe^0 dmpe dinitrogen complex (dmpe = 1,2-bis(dimethylphosphino)ethane) [3]. New insights into this chemistry have recently been obtained based on analogous iron complexes with the DMeOPrPE ligand (DMeOPrPE = 1,2-bis[bis(methoxypropyl)phosphino]ethane) [4]. Using this system the conversion of N_2 to ammonia and hydrazine with H_2 the reductant has been demonstrated.

In addition to these studies there has been a renewed interest in Fe dinitrogen chemistry based on mononuclear, coordinatively unsaturated systems which is inspired by the trigonal-pyramidal coordination of the iron centers in the iron molybdenum cofactor (FeMoco) of the enzyme nitrogenase [5]. Thus three-coordinate Fe complexes with nitrogen, sulfur and hydrogen ligands have been synthesized which exhibit a pronounced ability to cleave the N-N bonds of substrates like diphenylhydrazine and diphenyldiazene [6]. Four-coordinate iron phosphine systems of the type $L_3Fe\text{-}N_x$ have been shown to exhibit a high degree of redox flexibility and can accomodate both π-basic and π-acidic ligands [7]. These studies have led to the characterization of mono- and dinuclear Fe-N_2 complexes one of which, an Fe^0 system, could be alkylated at the N_2 ligand, a reaction that is related to protonation. More recently iron complexes with neutral NP_3 and NS_3 ligands were prepared and the six-coordinate, diamagnetic dinitrogen complex $[Fe(N\text{-}P^iPr_3(N_2)(H)]PF_6$ was isolated and characterized [7c].

Analogous Fe^{II} hydrido-N_2 complexes with diphosphine coligands have been known for a long time [8]. These systems allow to obtain information about the influence of equatorial and *trans*-axial ligands on the bonding of N_2 to transition-metal centers, the very first step of nitrogen fixation. With this in mind we prepared Fe^{II} depe and dppe complexes with hydrido and halide coligands and explored the reactivity of the resulting class of compounds with respect to N_2 (depe = 1,2-bis(diethylphosphino)ethane; dppe = 1,2-bis(diphenylphosphino)ethane). In particular, we performed a structural and spectroscopic investigation of the complexes $[FeX(N_2)(depe)_2]BPh_4$ (X=Cl, Br) which have Fe-N_2 bonds that are both thermally and photochemically labile [9]. The bonding of N_2 in these systems pro-

---

Prof. Dr. F. Tuczek
Inst. Für Anorgan. Chemie der Universität
Otto-Hahn-Platz 6/7
D-24098 Kiel.
email: ftuczek@ac.uni-kiel.de

ceeds in a spin-forbidden process which could be shown to be the origin of the lability of the Fe-N_2 bond. The analogous Fe^{II}-N_2 depe complex with a *trans* hydrido ligand is thermally more stable [10]. This also applies to the corresponding dppe system $[FeH(N_2)(dppe)_2]^+$; the five-coordinate precursor $[FeH(dppe)_2]BPh_4$ has even been described to bind dinitrogen in tetrahydrofuran (thf) solution from air [11]. $[FeCl(depe)_2]^+$, in contrast, is extremely oxygen sensitive in solution [12]. These differences in reactivity must be correlated with different electronic ground states which we determine by a combination of magnetic susceptibility measurements, various spectroscopic methods and quantum-chemical calculations.

Recently we reported a vibrational-spectroscopic comparison between $[FeCl(N_2)(depe)_2]BPh_4$ and $[FeH(N_2)(depe)_2]BPh_4$ coupled to normal coordinate analysis [10]. In agreement with the high values found for ν(NN) (2086 and 2091 cm^{-1}, respectively), the N_2 ligands in both compounds are non-activated which corresponds to the observation that N_2 is not protonatable in Fe^{II} systems (*vide supra*). Taking into account the short Fe-N bond lengths, the values of the Fe-N stretching force constants (2.58 mdyn/Å and 2.55 mdyn/Å, respectively) were found to be compatible with those of other Fe^{II} low-spin compounds coordinated to backbonding, N-coordinating ligands. Moreover, the force fields obtained for the Fe-N_2 units of both compounds were found almost identical. Nevertheless, the thermal stability of these systems with respect to loss of N_2 is different. This indicates that the Fe-N potentials are at the equilibrium positions unaffected by possible ground-state level crossing processes which occur at larger metal-N_2 distances and may influence the thermal stability of the N_2-adduct.

Herein we present a complementary study of the iron(II) hydrido complexes $[Fe(H)(dppe)_2]BPh_4$ (**1**) and $[Fe(H)(N_2)(dppe)_2]BPh_4$ (**2**) which are characterized by Mössbauer, NMR, UV/Vis, infrared, and Raman spectroscopies as well as magnetic susceptibility measurements, coupled to DFT calculations. In addition to the homogeneous reaction with dinitrogen in thf, complex **1** has been known to also bind N_2 in the solid state [11]. In the present investigation we monitor this process spectroscopically and compare it to the binding of N_2 by **1** in solution. The general implications of these results with respect to the bonding of dinitrogen to iron diphosphine complexes are discussed.

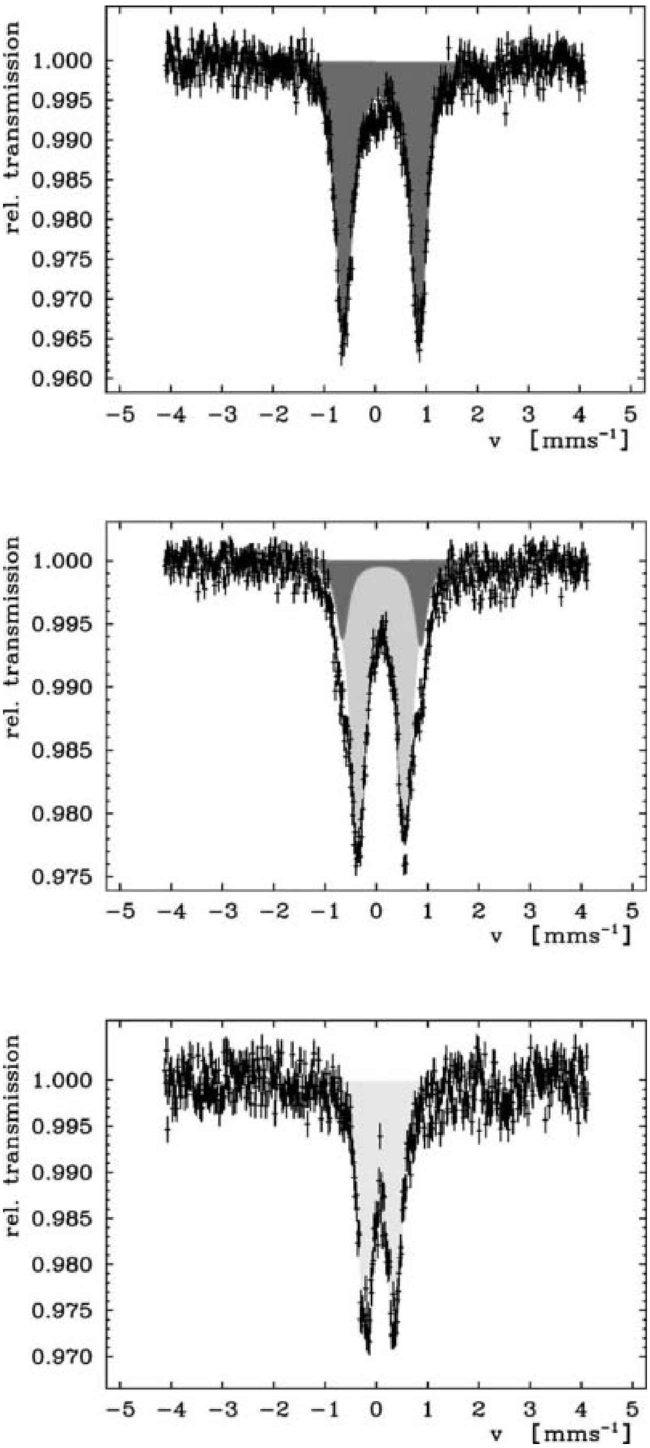

Fig. 1 Mössbauer spectra of blue $[FeH(dppe)_2]BPh_4$ (**1**) (top), green $[FeH(N_2)(dppe)_2]BPh_4$ (**2b**) (middle) and yellow $[FeH(N_2)(dppe)_2]BPh_4$ (**2a**) (bottom) at 150 K.

Results and Analysis

Mössbauer Spectroscopy and Magnetic Susceptibility

In agreement with the literature [11], the blue compound $[FeH(dppe)_2]BPh_4$ (**1**) binds dinitrogen in thf solution to give yellow $[FeH(N_2)(dppe)_2]BPh_4$ (**2a**). Moreover, it has been reported in ref. [11] that **1** reacts with N_2 in the solid state. We found that exposure of **1** to 1 atm of nitrogen does not give yellow **2a** but leads to a green compound **2b**. The colour of **2b** does not change to yellow after several months of storage under dinitrogen but remains green. Importantly, the N_2 compounds **2a** and **2b** are not only different in their colour but also differ in their other physical properties, as shown below.

Comparative Mössbauer spectra of **1**, **2a** and **2b** taken at 150 K are presented in Figure 1. Obviously these compounds exhibit doublets which have about equal chemical

Table 1 Mössbauer and magnetic parameters of $[FeH(dppe)_2]BPh_4$ (**1**) and $[FeH(N_2)(dppe)_2]BPh_4$ (**2a/2b**).

Complex	δ^a	$\Delta E_Q{}^a$	$\mu_{eff}{}^b$ (solid state)	$\mu_{eff}{}^c$ (in solution)
$[FeH(dppe)_2]BPh_4$ (**1**)	0.227(4)	1.527(8)	2.9	diamagnetic
$[FeH(N_2)(dppe)_2]BPh_4$ (**2a**)	0.183(7)	0.562(12)	diamagnetic	diamagnetic
$[FeH(N_2)(dppe)_2]BPh_4$ (**2b**)	0.209(5)	0.905(14)	2.9	diamagnetic

[a] measured at 150 K. [b] value for μ_{eff} at room temperature. [c] measured in thf at room temperature.

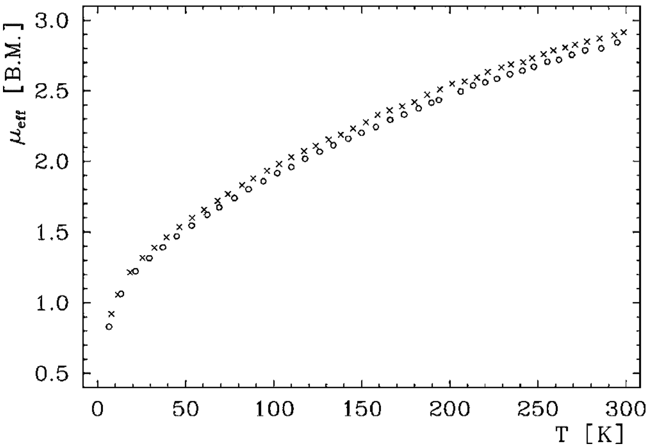

Fig. 2 Effective magnetic moment μ_{eff} in μ_B of $[FeH(dppe)_2]BPh_4$ (**1**) (x) and green $[FeH(N_2)(dppe)_2]BPh_4$ (**2b**) (o) vs temperature (K).

shifts but differ with respect to their quadrupole splittings (see also Table 1). In particular, the quadrupole splitting of $[FeH(N_2)(dppe)_2]^+$ is larger in green **2b** (ΔE_Q = 0.905(14) mm/s) than in yellow **2a** (ΔE_Q = 0.562(12) mm/s) and thus indicates that the green colour of **2b** does not result from a physical mixture of blue **1** and yellow **2a**. The coordination unit of compound **2b** therefore must have an electronic and structure which is different to that of compound **2a**. However, the solid-state reaction of **1** with N_2 leading to compound **2b** is not complete as the spectrum of **2b** shows a second doublet of ~20 % of the total intensity (δ_{IS} = 0.212(14) mm/s; ΔE_Q = 1.528(35) mm/s at T = 150 K). The Mössbauer parameters of this doublet are almost identical to those of the five-coordinate complex **1** prepared independently (δ_{IS} = 0.227(4) mm/s; ΔE_Q = 1.527(8) mm/s at T = 150 K). The second doublet in the spectrum of **2b** is therefore assigned to the dinitrogen-free precursor **1**.

To further characterize the five-coordinate species **1** and the corresponding N_2 complexes **2a** and **2b**, magnetic susceptibility data were recorded. Whereas compound **2a** generated by the solution reaction of $[FeH(dppe)_2]^+$ with N_2 was found to be diamagnetic, compound **2b** turned out to be paramagnetic. Figure 2 shows the effective magnetic moment μ_{eff} of **1** (x) and **2b** (o) as a function of temperature. With a room temperature μ_{eff} value of 2.9 μ_B which corresponds to the spin-only value for a triplet, the ground state spin of **1** must be S = 1, representing the "intermediate" spin state for Fe^{II}. Importantly, the μ_{eff} vs. T curve of **2a** is practically identical to that of **1**, indicating that the binding of N_2 has no influence on the magnetic properties of **1**. This surprising result is interpreted below with the help of DFT calculations.

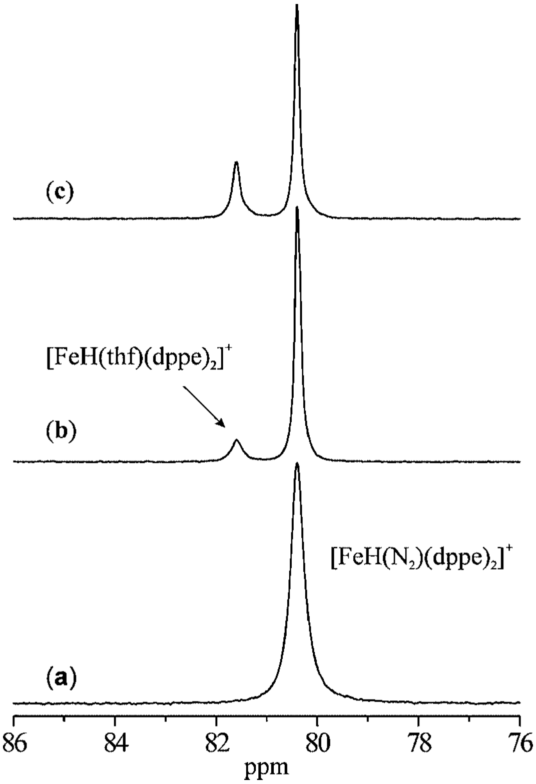

Fig. 3 (a) ^{31}P-NMR spectra of *trans*-$[FeH(N_2)(dppe)_2]BPh_4$ (**2a**) in thf-d_8 at room temperature. (b,c) The additional peak at 81.6 ppm increasing in intensitiy with the time is assigned to the species *trans*-$[FeH(thf)(dppe)_2]^+$, where the N_2 ligand is exchanged by a thf solvent molecule.

NMR spectroscopy

The ^{31}P NMR spectrum of the dinitrogen complex **2a** is displayed in Figure 3a. It exhibits a singlet at 80.4 ppm which is due to the four equivalent phosphorus atoms (Table 2). Interestingly, another singlet at 81.6 ppm is observed when the same solution is remeasured after 18 hours (Figure 3b). An additional measurement after 42 hours shows that the intensity of this signal has further increased while the intensity of the first detected peak has further decreased (Figure 3c). The corresponding ^1H NMR spectrum (Figure 4) exhibits two quintets at −15.6 and −29.4 ppm the former of which is assigned to the hydrido ligand of **2a**. The latter increases with time and therefore corresponds to the ^{31}P signal at 82.4 ppm in Figure 3c. These signals are attributed to the dinitrogen-free complex **1** because the same peaks are observed in the NMR spectrum of **1** in thf. Under this condition the unsaturated five-

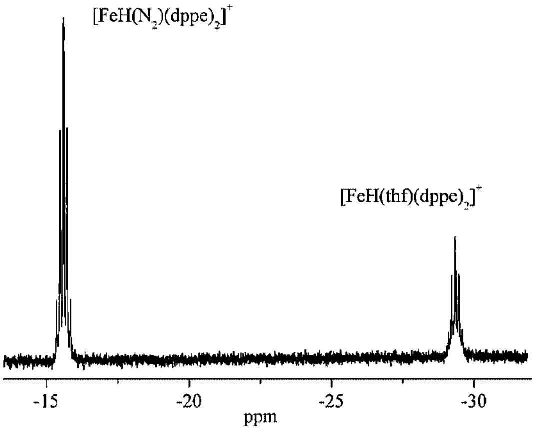

Fig. 4 ^{1}H-NMR spectrum of *trans*-[FeH(N$_2$)(dppe)$_2$]BPh$_4$ (**2a**) in thf-d_8 at room temperature, corresponding to the ^{31}P-NMR spectrum of **2a** measured after 42 hrs (Figure 3c). The peak at −29.4 ppm is assigned to the species *trans*-[FeH(thf)(dppe)$_2$]$^+$, where the N$_2$ ligand is exchanged by a thf solvent molecule.

Table 2 NMR parameters of [FeH(^{15}N$_2$)(dppe)$_2$]BPh$_4$ (**2a**) and [FeH(dppe)$_2$]BPh$_4$ (**1**)

Complex	δ^1H	δ^{31}P	δ^{15}N$_\alpha$	δ^{15}N$_\beta$	*J* (Hz)	
[FeH(N$_2$)(dppe)$_2$]BPh$_4$ (**2a**)	−15.6	80.4	−61.8	−38.9	$^2J_{HP}$	48.0
					$^2J_{HN\alpha}$	5.9
					$^3J_{HN\beta}$	3.2
					$^1J_{NN}$	3.6
					$^2J_{PN\alpha}$	~2
					$^3J_{PN\beta}$	≤0.2
[FeH(dppe)$_2$]BPh$_4$ (**1**)	−29.3	81.6	–	–	$^2J_{HP}$	49.0

coordinate complex **1** is coordinated with a thf solvent molecule, forming the species *trans*-[FeH(thf)(dppe)$_2$]$^+$ (see below). These results therefore indicate that **2a** is not stable in coordinating solvents like thf with respect to substitution of the N$_2$ ligand.

The ^{31}P NMR (^{1}H coupled) spectrum of the parent complex **1** was measured in thf in the temperature range from 213 K to 333 K (Figure 5). The solution was first cooled down from room temperature to 213 K (Figure 5a); at this temperature the spectrum exhibits two doublets at 81.6 and 80.4 ppm. As mentioned before, the peak at 81.6 ppm is associated with the solvent-coordinated complex *trans*-[FeH(thf)(dppe)$_2$]$^+$ whereas the peak at 80.4 ppm is caused by a contamination with the corresponding N$_2$ complex$^{1)}$. The intensity of the latter signal decreases when the temperature is raised to 273 K (Figures 5b-d), which can be attributed to thermal loss of the N$_2$ ligand. Upon further heating, the peak broadens at 293 K and starts shifting upfield (e; *vide infra*). Further heating leads to disappearance of this signal (f-h). When the solution is cooled down to 213 K again (Figures 5i,j), only the species corresponding to *trans*-[FeH(thf)(dppe)$_2$]$^+$ is detected$^{2)}$. The N$_2$ ligand of the impurity **2a** of **1** therefore has been completely replaced by thf in the course of the described thermal cycle.

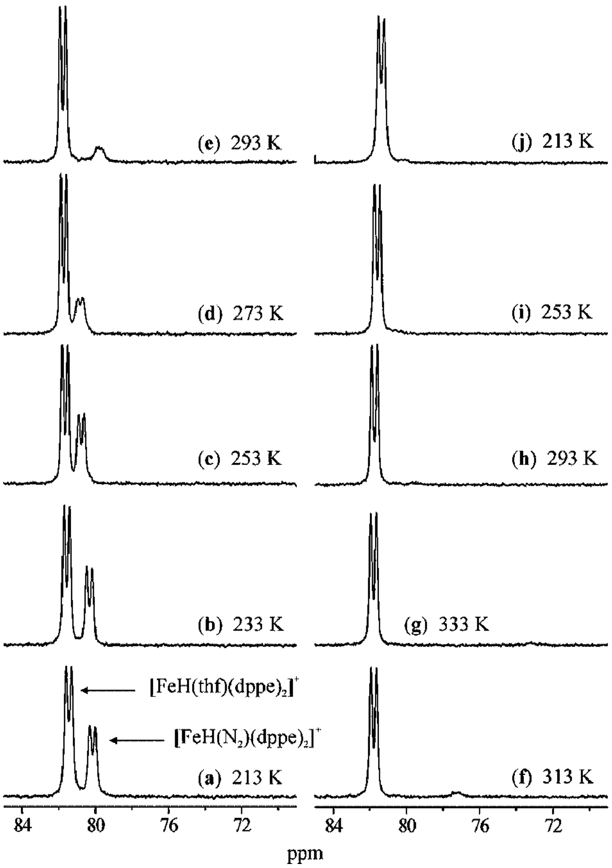

Fig. 5 ^{31}P-NMR spectra of [FeH(dppe)$_2$]BPh$_4$ (**1**) in thf-d_8, measured in the temperature range from 213 K up to 333 K (a-f) and back to 213 K (g-j).

Vibrational Spectroscopy

Sections of the Raman and IR spectra of complexes **1**, **2b**, **2a** and the ^{15}N-substituted isotopomer of **2a** are given in Figure 6 (a), (b), (c) and (d), respectively. Vibrational frequencies of all compounds are collected in Table 3. The N-N stretch of yellow **2a** is observed at 2122 cm^{-1} in the natural isotope spectrum (c) and upon ^{15}N substitution shifts to 2052 cm^{-1} (d). In the Raman spectrum this feature is found at 2124 cm^{-1} (^{15}N: 2053 cm^{-1}). In agreement with this high value of ν(NN), the N$_2$ ligand in **2a** is *non-activated* which corresponds to the observation that N$_2$ is not protonatable in Fe^{II} systems [1, 2]. The IR spectrum of green **2b** (Fig.6b) shows the N-N stretch at 2120 cm^{-1}. In addition, a much sharper band appears at 2145 cm^{-1} which is found as the

---

1) It is difficult to prepare a solution of **1** in complete absence of N$_2$ as **1** even binds N$_2$ from argon containing N$_2$ in ppm amounts.

2) Determination of peak hights (thermally corrected) indicate that the concentration of the thf complex remains constant in the course of the cooling process.

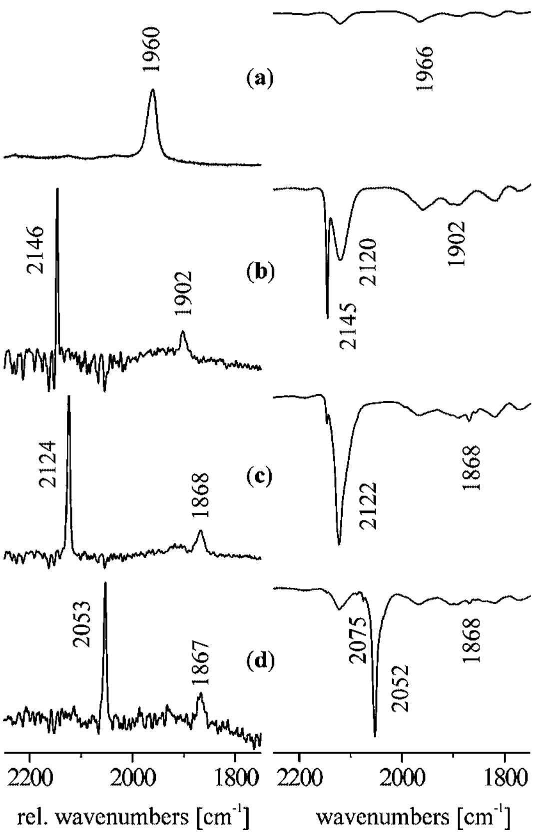

Fig. 6 Raman (left) and IR spectra (right) of (a) $[FeH(dppe)_2]BPh_4$ (**1**), (b) green $[FeH(N_2)(dppe)_2]BPh_4$ (**2b**), (c) yellow $[FeH(N_2)(dppe)_2]BPh_4$ (**2a**) and (d) $FeH(^{15}N_2)(dppe)_2]BPh_4$.

Table 3 Vibrational frequencies /cm^{-1} of $[FeH(dppe)_2]BPh_4$ (**1**) and $[FeH(N_2)(dppe)_2]BPh_4$ (**2a/2b**).

Complex		ν(NN)	ν(FeH)
$[FeH(dppe)_2]BPh_4$ (**1**)		–	1960
$[FeH(N_2)(dppe)_2]BPh_4$ (**2b**)	nat. isot.	2145	1902
	$^{15}N_2$	2075	1902
$[FeH(N_2)(dppe)_2]BPh_4$ (**2a**)	nat. isot.	2122	1868
	$^{15}N_2$	2052	1867

dominant peak in the Raman spectrum at 2146 cm^{-1}. Interestingly, the latter spectrum exhibits no peak at ~2120 cm^{-1}. An explanation for this observation is that the IR spectrum of **2b** is measured on pellets obtained by grinding of the compound with RbI, followed by application of pressure. This generates a "solid solution" of **2b** in the matrix of the alkali halide pellet with the N-N stretch of the corresponding dinitrogen complex being located at the same position as in yellow **2a**. The Raman spectrum of **2b**, in contrast, is obtained from the neat compound without application of pressure and thus provides the "true" N-N stretching frequency of crystalline, green **2b** [3].

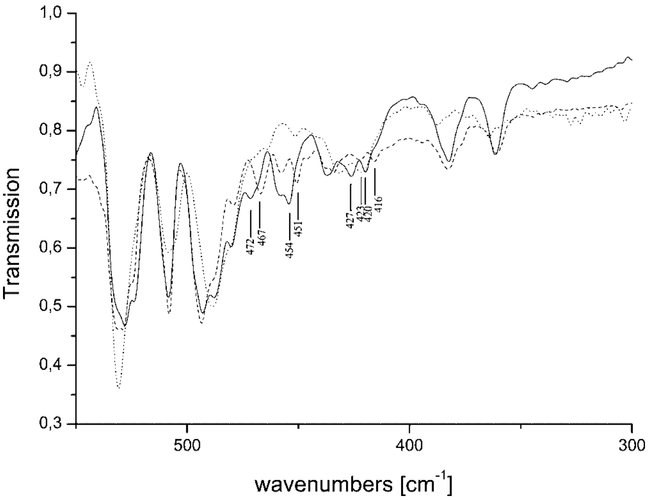

Fig. 7 Far-infrared spectra of $[FeH(N_2)(dppe)_2]BPh_4$ (**2a**, solid line), $[FeH(^{15}N_2)(dppe)_2]BPh_4$ (**2a**, dashed line) and $FeH(dppe)_2]BPh_4$ (**1**, dotted line), with positions of bands shifting upon isotope substitution

Experimental identification of the metal-N_2 ligand vibrations is difficult. Figure 7 shows that there are four vibrations in the IR spectrum of **2a** below 500 cm^{-1}; i.e., at 472/454 cm^{-1} and 427/420 cm^{-1}, which shift in the ^{15}N spectrum to 467/451 cm^{-1} and 423/416 cm^{-1}, respectively. However, a definitive assignment of these vibrations to ν(FeN) and δ(FeNN), as achieved for $[FeH(N_2)(depe)_2]BPh_4$ and $[FeCl(N_2)(depe)_2]BPh_4$ [10], is problematic. In case of the latter compounds, the stretch could be distinguished from the bend by its much higher intensity in the Raman spectrum. The Raman spectra of **2a**, however, are not resolved well enough to provide this information (data not shown). Irrespective of the detailed assignment, it nevertheless can be stated that both Fe-N_2 metal-ligand vibrations of **2a** are at *lower* frequency than in $[FeH(N_2)(depe)_2]BPh_4$ and $[FeCl(N_2)(depe)_2]BPh_4$ where ν(FeN) is found at 479 and 503 cm^{-1} and δ(FeNN) at 487 and 518/512 cm^{-1}, respectively. This corresponds to the observation that the N-N stretching frequency of **2a** (2122 cm^{-1}) is *higher* than both in $[FeH(N_2)(depe)_2]BPh_4$ (2091 cm^{-1}) and $[FeCl(N_2)(depe)_2]BPh_4$ (2086 cm^{-1}) [10].

More information on the binding of N_2 is obtained from the Fe-H stretching vibration. The Fe-H stretch of **1** is observed in the IR and the Raman spectra at 1966 cm^{-1} and 1960 cm^{-1}, respectively (Fig.6a). The frequency of this band is lowered to 1902 cm^{-1} upon reaction with dinitrogen in the solid state, giving the green product **2b** (Fig.6b). In the spectra of the solution product **2a**, in contrast, ν(FeH) is found at 1868 cm^{-1} (Fig.6c), shifting upon ^{15}N substitution to 1867 cm^{-1} (Fig.6d). The frequency of the Fe-H stretching vibration in the green compound (**2b**) thus indicates an *intermediate* position of N_2 bonding between the uncoordinated precursor **1** and the solvent-reacted product **2a**. The fact that N_2 is bound less firmly in **2b** than

---

[3] To a slight extent, the sharp band at 2145 cm^{-1} is also visible in the IR spectrum of yellow **2a** and its ^{15}N isotopomer (2075 cm^{-1}).

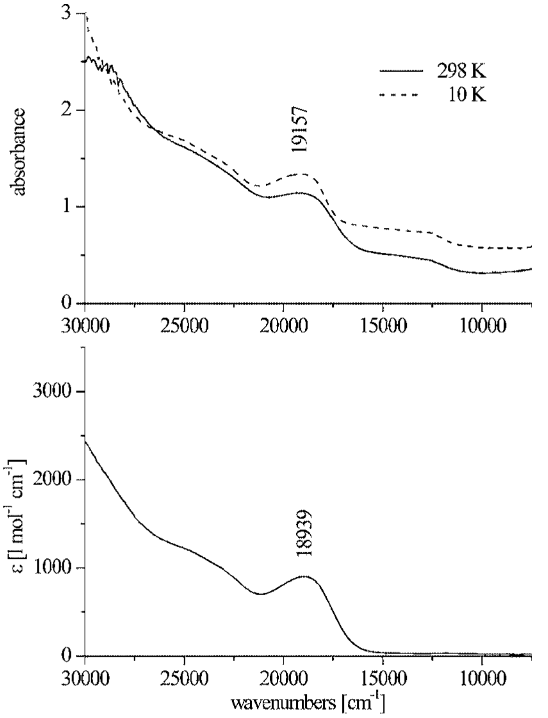

Fig. 8 UV-vis spectra of $[FeH(N_2)(dppe)_2]BPh_4$ (**2a**); top: obtained on solid mulls between sapphire windows; bottom: measured in thf at room temperature.

in **2a** is also reflected by the higher N-N frequency in the former as compared to the latter compound.

Optical absorption spectroscopy

Optical absorption spectra of the dinitrogen complex **2a** both in the solid state and in thf solution are displayed in Figure 8. In the visible region both spectra are dominated by an intense band at ~19000 cm^{-1} with a molar decadic absorption coefficient ε of about 1000 M^{-1} cm^{-1}. Due to its high intensity it is not assigned to an Fe^{II} ligand-field (LF) transition, but to a hydride → Fe charge transfer transition[4)].

The optical absorption spectra of **1** in the solid state and in thf are displayed in Figure 9. The Vis/NIR part of the solid-state spectrum is dominated by an intense band at ~17000 cm^{-1}. Moreover, the solution spectrum is markedly temperature-dependent. The low-temperature (273 K) spectrum exhibits an intense band at ~19000 cm^{-1}, in analogy to the spectrum of the dinitrogen complex **2a** (Fig.8). Upon an increase of temperature the intensity of this band decreases and a new absorption band appears at ~15000 cm^{-1}. The colour of the solution thereby changes from red violet to blue violet. This colour change has been described in the literature [11] and ascribed to the temperature-dependent equilibrium

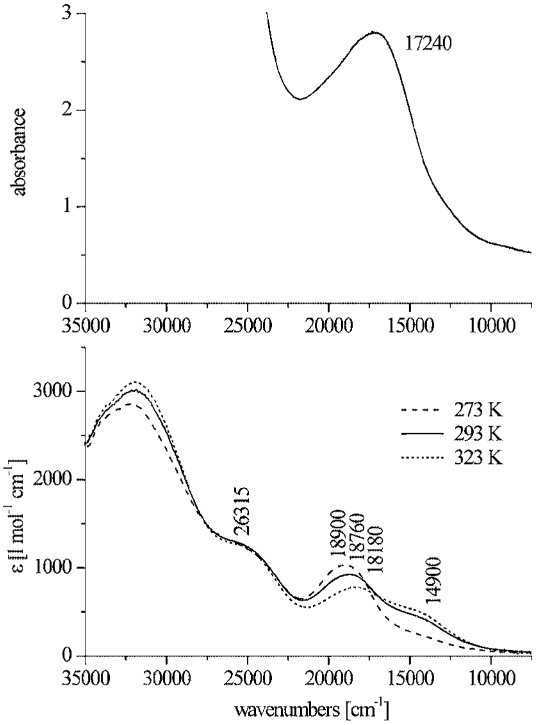

Fig. 9 UV-vis spectra of $[FeH(dppe)_2]BPh_4$ (**1**); top: obtained on solid mulls between sapphire windows at 10 K; bottom: measured in thf at 273 K (dashed line), 295 K (solid line) and 323 K (dotted line)

$$[FeH(thf)(dppe)_2]^+ \leftrightarrow [FeH(dppe)_2]^+ + thf \qquad (2).$$

The variable-temperature NMR results presented above, on the other hand, have clearly shown that the thf complex in the absence of N_2 gives a peak that is constant in intensity and position. A temperature dependence is only observed by NMR for the dinitrogen complex **2**, showing that N_2 is thermally labile and slowly exchanged by the solvent, especially at elevated temperatures. We thus conclude that the colour change of the thf solution of **1** is not due to loss of thf according to (2) but to a contamination with the N_2 complex which is converted to the thf complex. The colour change is therefore due to the ligand exchange reaction

$$[FeH(N_2)(dppe)_2]^+ + thf \xrightarrow{\Delta} [FeH(thf)(dppe)_2]^+ + N_2 \qquad (3).$$

The band at ~15000 cm^{-1} observed in the spectrum of **1** in thf at 323 K thus represents the true absorption of the thf complex of **1**.

Quantum-chemical (DFT) calculations

The results presented in the preceding sections have shown that $[FeH(dppe)_2]^+$ is able to bind dinitrogen in solution

---

[4)] These low-energy, high-intensity bands are found in all Fe^{II} hydrido complexes and disappear upon exchange of hydride by halide or dinitrogen; O. Franke, PhD Dissertation Christian Albrechts Universität Kiel, 2004.

Table 4 Energies of the optimized structure $\tilde{\text{I}}$ obtained with various methods

[Fe(diphos)$_2$H]$^+$ ($\tilde{\text{I}}$) Method	**Spinstate**	**Energy** [Hartree]	ΔE = E(Singlet) − E(Triplet)	
			[cm^{-1}]	[kcal/mol]
B3LYP/LanL2DZ	S = 0	−311.782232	+2063	+5.9
	S = 1	−311.791632		
B3LYP/TZVP	S = 0	−2791.770468	+205	+0.6
	S = 1	−2791.771402		
BP86/LanL2DZ	S = 0	−312.008174	−2331	−6.7
	S = 1	−311.997552		
BP86/TZVP	S = 0	−2792.052336	−4679	−13.4
	S = 1	−2792.031015		

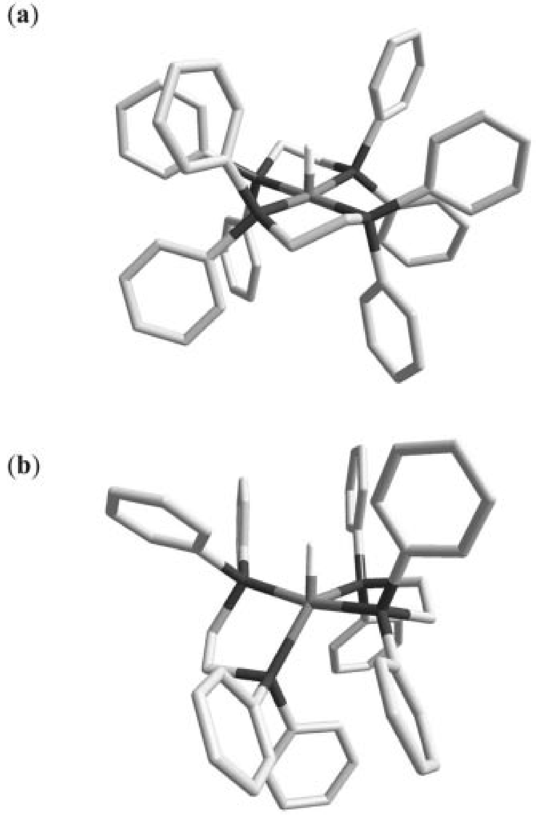

Fig. 10 Optimized structures of [FeH(dppe)$_2$]BPh$_4$ (**1**). (a) singlet ground state. (b) triplet ground state. Hydrogen atoms left for clarity.

and in the solid state, leading to two distinct dinitrogen adducts, yellow [FeH(N$_2$)(dppe)$_2$]$^+$(BPh$_4$) (**2a**) and green [FeH(N$_2$)(dppe)$_2$]+(BPh$_4$) (**2b**). Apart from their different Mössbauer, optical absorption and vibrational spectra, **2a** is diamagnetic and **2b** paramagnetic. As the parent compound [FeH(dppe)$_2$]$^+$BPh$_4$ (**1**) is paramagnetic as well, the reaction of **1** with N$_2$ in the solid state would provide a unique example for binding of N$_2$ to an iron complex in a triplet state. The S=1 ground state of the dinitrogen adduct **2b** is further remarkable as solution measurements of [FeH(N$_2$)(dppe)$_2$]$^+$ indicate an S=0 ground state. We therefore assume that the described bonding of N$_2$ in the triplet state is a solid-state effect.

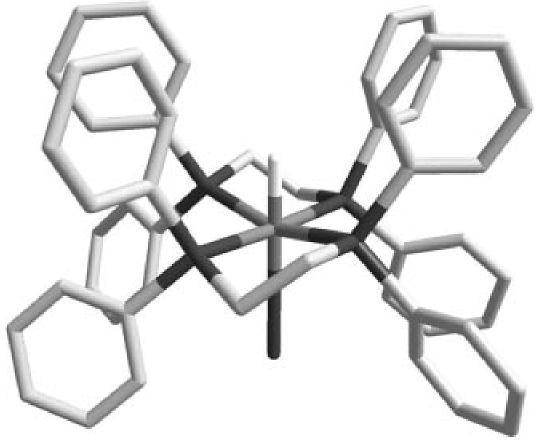

Fig. 11 Optimized structure of [FeH(N$_2$)(dppe)$_2$]BPh$_4$ (**2a**). Hydrogen atoms left for clarity.

Table 5 Energies of the optimized structures of [FeH(dppe)$_2$]$^+$ (**I**) and [FeH(N$_2$)(dppe)$_2$]$^+$ (**II**)

Model	Energy [Hartree]
[FeH(dppe)$_2$]$^+$ (**I**) (S=0)	−4638.415067
[FeH(dppe)$_2$]$^+$ (**I**) (S=1)	−4638.399448
[FeH(N$_2$)(dppe)$_2$]$^+$ (**II**) (S=0)	−4747.907322

Table 6 Bonding parameters of the optimized structures of [FeH(dppe)$_2$]$^+$ (**I**) and [FeH(N$_2$)(dppe)$_2$]$^+$ (**II**)

Complex	Bond lengths /Å						
	Fe-P(1)	Fe-P(2)	Fe-P(3)	Fe-P(4)	Fe-H	Fe-N	N-N
[FeH(dppe)$_2$]$^+$ (**I**) (S=1)	2.35	2.23	2.39	2.27	1.56	–	–
[FeH(dppe)$_2$]$^+$ (**I**) (S=0)	2.25	2.26	2.25	2.26	1.48	–	–
[FeH(N$_2$)(dppe)$_2$]$^+$ (**II**) (S=0)	2.31	2.29	2.31	2.29	1.53	1.81	1.14

In contrast to the paramagnetism observed for the solid precursor **1**, no direct evidence for a paramagnetic, five coordinate complex [FeH(dppe)$_2$]$^+$ was obtained in thf solution. Under these circumstances, however, this cation is coordinated by a solvent molecule and *therefore* diamagnetic.

In order to obtain information on the electronic ground state of *non-solvated* $[FeH(dppe)_2]^+$, DFT gas-phase calculations were performed [13]. The phenyl substituents of the dppe ligands were first substituted by hydrogen atoms, leading to the model $[FeH(diphos)_2]^+$ ($\tilde{\mathbf{I}}$) (diphos = H_2P-CH_2-CH_2-PH_2). Two functionals (B3LYP, BP86) and two basis sets (LanL2DZ and TZVP) were employed; the results are collected in Table 4. Evidently B3LYP predicts a triplet and BP86 a singlet groundstate for $\tilde{\mathbf{I}}$. This result derives from the fact that Hartree-Fock exchange is (in contrast to BP86) admixed in B3LYP, which acts to favor the triplet state. From prior experience with calculations on iron complexes we assume that for the iron complex **1** the B3LYP functional is superior to BP86 with respect to predicting the relative energies of the singlet and the triplet states [9]. Furthermore, as the TZVP is superior to the LanL2DZ basis set, it results from Table 4 that singlet and triplet of $\tilde{\mathbf{I}}$ are about isoenergetic. Exchanging the hydrogen atoms of $\tilde{\mathbf{I}}$ by phenyl or alkyl groups or modifying the geometry of $\tilde{\mathbf{I}}$ by packing effects will therefore determine whether the ground state spin of **1** is 0 or 1.

Unfortunately, no crystal-structure information is available for **1**. In order to obtain an impression of the geometries of **1** in the singlet and triplet states, DFT calculations have been performed on the full molecule (**I**)[5]. The corresponding energies are given in Table 5; characteristic bond lengths are collected in Table 6. In agreement with the calculations performed on the simplified model $\tilde{\mathbf{I}}$ the singlet state of **I** has a quadratic-pyramidal geometry (Figure 10a). This geometry is retained in the corresponding (S=0) dinitrogen adduct **II**, with the N_2 ligand arranged in *trans*-position to the hydride (Figure 11). The corresponding S=1 dinitrogen adduct could not be converged, thus leaving the question of the geometry of $[FeH(N_2)(dppe)_2]^+$ in compound **2b** open (see Discussion). In the triplet state of the five-coordinate precursor **I**, one phosphine ligand is rotated out of the P_4 plane, generating a geometry intermediate between quadratic-pyramidal and trigonal-bipyramidal (Figure 10b). The same geometry has been obtained for the triplet state of the simplified model $\tilde{\mathbf{I}}$, independently of the method employed, such that it can be assumed that this structure is an inherent property of the S=1 $FeHP_4$ unit.

Discussion

The goals of the investigations described in the preceding sections were to elucidate the electronic structure of the five-coordinate complex $[Fe(H)(dppe)_2]^+$ (**1**) and determine the structural and spectroscopic consequences of its reaction with N_2. In agreement with literature data, **1** has been found to react with N_2 in solution and in the solid state. In our hands, these reactions lead to the yellow and green products **2a** and **2b**, respectively. Although the solid-state reaction of **1** with N_2 generating **2b** does not proceed to 100 %, it clearly can be stated that **2a** and **2b** differ in their physical and spectroscopic properties. Moreover, the five-coordinate dppe precursor complex **1** is found to be paramagnetic in the solid state whereas in solution it is diamagnetic. DFT calculations indicate that the singlet and triplet states of $[FeH(dppe)_2]^+$ are about isoenergetic, thus principally accounting for the paramagnetism of this compound in the solid state. Geometry optimization of the triplet state leads to a molecular geometry where one phosphine donor is bent out of the equatorial plane.

Experimentally, the triplet configuration of $[Fe(H)(dppe)_2]^+$ is retained if N_2 is bound in the solid state, leading to compound **2b**. Although no DFT information could be obtained on S=1 $[FeH(N_2)(dppe)_2]^+$, general chemical experience strongly suggests that the relaxed geometry of a hydrido-N_2 complex with a tetraphosphine coordination is associated with a singlet ground state. This is in fact experimentally observed for the product of the homogeneous reaction of **1** with N_2 in thf, giving diamagnetic, yellow $[Fe(H)(N_2)(dppe)_2]^+$ (**2a**). The triplet state of the dinitrogen adduct in **2b** therefore must be a consequence of steric constraints in the solid state which preclude the attainment of the gas-phase equilibrium geometry.

Only speculations can be made regarding the geometry of the paramagnetic dinitrogen adduct in green $[Fe(H)(N_2)(dppe)_2]^+$ (**2b**) resulting from the solid-state reaction of **1** with N_2. If the N_2-ligand in **2b** is bound in a *trans* position to hydride as in **2a**, two of the phosphine ligands could be bent away from the equatorial P_4 plane to generate a triplet ground state. Due to the unfavourable disposition of the phosphine ligands, the Fe-N_2 bond has to be elongated in this structure with respect to equilibrium configuration present in **2a** (Scheme 1).

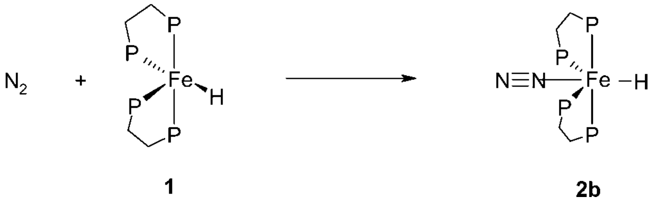

Scheme 1

Experimental evidence for the corresponding weakening of the metal-N_2 interaction is provided by the higher value of ν(NN) and the much narrower linewidth of the corresponding band in the IR spectrum of **2b** in comparison to that of **2a**. In terms of Mössbauer quadrupole splittings, **2b** lies between the dinitrogen-free precursor **1** and the yellow dinitrogen complex **2a** which also reflects an intermediate position of **2b** in the reaction coordinate of **1** leading to the diamagnetic complex **2a**. It thus appears that the dinitrogen ligand in **2b** is bound at a comparatively large distance from the iron atom and would further move towards the metal center if the phosphine ligands were not fixed at their positions.

---

[5] Functional BP86, Basis set LanL2DZ

Another sensitive probe of the electronic and geometric structure of these systems is provided by the spectroscopic signatures of the Fe-H interactions. Upon coordination of N_2 in *trans* position the Fe-hydride interaction is weakened, which is evident from the lowering of the Fe-H stretching vibration. Also in terms of Fe-H stretching frequencies, complex **2b** is intermediate between **1** and **2a**, supporting the above conclusions. Fe-H bonding is further reflected by intense low-energy transitions visible in the electronic absorption spectrum which we attribute to hydride → Fe CT transitions. For dinitrogen and thf coordinated [Fe(H)(dppe)$_2$]$^+$ the hydride → Fe CT transition is found at ~19000 and ~15000 cm^{-1}, respectively, whereas in paramagnetic, solid [FeH(dppe)$_2$]BPh$_4$ it is located at ~17000 cm^{-1}.

In summary, the electronic structure of the Fe^{II} hydrido complex [FeH(dppe)$_2$]$^+$ (**1**) has been defined and a detailed understanding of its reactions with N_2 leading to the yellow and green dinitrogen adducts **2a** and **2b** has been achieved. This completes our investigations on the binding of N_2 to Fe^{II} diphosphine complexes with different trans ligands X (X=H, Hal). Notably, three types of reactions with N_2 have been established: spin-allowed S=0 → S=0 for [FeH(dppe)$_2$]$^+$ → [FeH(N$_2$)(dppe)$_2$]$^+$ in solution; spin-allowed S=1 → S=1 for [FeH(dppe)$_2$]$^+$ → [FeH(N$_2$)(dppe)$_2$]$^+$ in the solid state and spin-forbidden S=1 → S=0 for [FeX(depe)$_2$]$^+$ → [FeX(N$_2$)(depe)$_2$]$^+$, X=Cl, Br. This class of compounds thus provides a textbook example for the fact that simple changes in the coordination sphere of transition-metal complexes can greatly influence their electronic structure and, correspondingly, their reactivity.

Experimental Section

Synthetic Procedures and Spectroscopic Measurements. Synthesis and handling of all compounds were performed under Argon or N_2 by use of Schlenk techniques and gloveboxes. All solvents were dried and freshly destilled under argon. The ligands 1,2-bis(diethylphosphino)ethane (depe) and 1,2-bis(diphenylphosphino)ethane (dppe) were obtained from Strem Chemicals; $^{15}N_2$ (98 %) was purchased from EURISO-TOP GmbH. All reagents were used without further purification. Sample manipulations for vibrational, UV/Vis- and NMR spectroscopy were performed in a glovebox. Mössbauer spectra were recorded with a WISSEL setup equipped with a He flow-through cryostat (Oxford CF506). Isomer shifts are given with respect to α-iron. Magnetic susceptibility was measured with a Physical Instruments (PI) vibrating sample (Foner) magnetometer at the Institute of Inorganic and Analytical Chemistry, University of Mainz. Susceptibility data were corrected for diamagnetic contributions using Pascal's constants. Susceptibility measurements in solution were performed by the Evans method. NMR spectra were recorded on a Bruker Avance 400 pulse Fourier transform spectrometer operating at a ^{1}H frequency of 400.13 MHz (^{31}P 161.98 MHz, ^{15}N 40.55 MHz) using a 5 mm inverse triple-resonance probe head. References as external standards: H_3PO_4 85 % pure, δ(^{31}P) 0 ppm; CH_3NO_2 neat, δ(^{15}N) 0 ppm. UV-vis spectra were measured with a Varian CARY 5 UV-vis-NIR spectrometer. Middle-infrared (MIR) spectra were obtained on RbI pellets using a Mattson Genesis Type I spectrometer. Far-infrared (FIR) spectra were measurd using a Bruker IFS66 spectrometer. Raman spectra with an irradiation at 1060 nm were recorded on a Bruker IFS 66/CS NIR FT-Raman spectrometer. The setup involves a 350 mW Nd-YAG-Laser with an excitation wavelength of 1064 nm. Samples were pressed as neat compounds into the groove of a sample holder which was sealed with a glass plate to ensure inert gas conditions. Raman spectra with excitation in the visible light range were performed on a DILOR XY spectrometer equipped with a closed-cycle cryostat and a CCD detector.

Synthesis of [FeH(dppe)$_2$]BPh$_4$ (1). This complex was prepared following the literature procedure [14]. Elemental Analysis: Theor. C 77.8, H 5.9; Found C 78.0, H 6.2 %.

Synthesis of [FeH(N$_2$)(dppe)$_2$]BPh$_4$ (2a/b). (a) Compound **2a** was initially synthesized by the following method: A solution of 400 mg (0.341 mmol) of **1** in 30 mL of thf was stirred for 3 hours under dinitrogen; the colour thereby changed from blue-green to red. The solvent was removed *in vacuo* and the residue taken up with 10 mL of dichloromethane. The remaining solid was removed by filtration and washed twice with 2 mL of dichloromethane. The combined filtrates were reduced by vacuum to a volume of 3 mL; subsequently 20 mL of diethyl ether were added slowly. The red precipitate was collected by filtration and dried *in vacuo*. Yield of **2a**: 170 mg (42 %). For the present study compound **2a** was prepared by the method described in (b) which was found to be superior to (a).

(b) A suspension of [FeH(dppe)$_2$]BPh$_4$ (**1**) (0.30 g, 0.25 mmol) in 10 mL of toluene was allowed to stir overnight at room temperature under 1 atm of nitrogen. The resulting yellow solid (**2a**) was separated by filtration and dried under vacuum. Elemental Analysis: Theor. C 76.0, H 5.8, N 2.3; Found C 74.3, H 5.5, N 1.9 %.

(c) [FeH(dppe)$_2$]BPh$_4$ (**1**) reacts with nitrogen in the solid state, resulting in a green compound (**2b**) after storing under 1 atm of nitrogen for several weeks. Elemental Analysis: Theor. C 76.0, H 5.8, N 2.3; Found C 73.7, H 5.8, N 0.9 %.

Acknowledgments. Financial support for this research has been provided by DFG and FCI. Assistance in the vibrational measurements bei *Uschi Cornelissen* is gratefully acknowledged. We thank *V. Ksenofontov* at Johannes Gutenberg University Mainz for performing the magnetic susceptibility measurements.

References

[1] (a) B. A. McKay, M. D. Fryzuk, *Chem. Rev.* **2004**, *104*, 385; (b) M. Hidai, Y. Mizobe, *Chem. Rev.* **1995**, *95*, 1115; (c) D. V. Yandulov, R. R. Schrock, *Science* **2003**, *76*, 301; (d) M. D. Fryzuk, S. A. Johnson, *Coord. Chem. Rev.* **2000**, *200−202*, 379; (e) M. Hidai, *Coord. Chem. Rev.* **1999**, *185−186*, 99; (f) R. A. Henderson, G. J. Leigh, C. J. Pickett, *Adv. Inorg. Chem. Radiochem.* **1983**, *27*, 197.

[2] F. Tuczek, N. Lehnert, *Angew. Chemie* **1998**, *110*, 2780; *Angew. Chem. Int. Ed.* **1998**, *37*, 2636.

[3] (a) G. J. Leigh, M. Jimenez-Tenorio, *J. Am. Chem. Soc.* **1991**, *113*, 5862; (b) A. Hills, D. L. Hughes, M. Jimenez-Tenorio, G. J. Leigh, A. T. Rowley, *J. Chem. Soc., Dalton Trans.* **1993**,

3041; (c) D. A. Hall, G. J. Leigh, *J. Chem. Soc., Dalton Trans.* **1996**, 3539.

[4] J. D. Gilbertson, N. K. Szymczak, D. R. Tyler, *J. Am. Chem. Soc.* **2005**, *127*, 10184.

[5] O. Einsle, F. A. Tezcan, S. L. A. Anrade, B. Schmid, M. Yoshida, J. B. Howard, D. C. Rees, *Science* **2002**, *297*, 1696.

[6] (a) P. L. Holland, *Can. J. Chem.* **2005**, *83*, 296−301; (b) J. M. Smith, R. J. Lachicotte, P. L. Holland, *J. Am. Chem. Soc.* **2003**, *125*, 15752; (c) J. M. Smith, R. J. Lachicotte, K. A. Pittard, T. R. Cundari, G. Lukat-Rodgers, K. R. Rodgers, P. L. Holland, *J. Am. Chem. Soc.* **2001**, *123*, 9222.

[7] (a) T. A. Betley, J. C. Peters, *J. Am. Chem. Soc.* **2003**, *125*, 10782; (b) T. A. Betley, J. C. Peters, *J. Am. Chem. Soc.* **2004**, *126*, 6252; (c) C. E. MacBeth, S. E. Harkins, J. C. Peters, *Can. J. Chem.* **2005**, *83*, 332.

[8] (a) G. M. Bancroft, J. J. Mays, B. E. Prater, *J. Chem. Soc. Chem. Commun.* **1969**, 585; (b) I. E. Buys, L. D. Field, T. W. Hambley, A. E. D. McQueen, *Acta Crystallogr.* **1993**, *C49*, 1056; (c) H. Azizian, R. H. Morris, *Inorg. Chem.* **1983**, *22*, 6; (d) A. Hills, D. L. Hughes, M. Jimenez-Tenorio, G. J. Leigh, *J. Organomet. Chem.* **1990**, *391*, C41.

[9] O. Franke, B. E. Wiesler, N. Lehnert, C. Näther, J. Neuhausen, V. Ksenofontov, F. Tuczek, *Inorg. Chem.* **2002**, *41*, 3491.

[10] O. Franke, B. E. Wiesler, N. Lehnert, F. Tuczek, *Z. Anorg. Allg. Chem.* **2002**, *628*, 2395.

[11] (a) P. Giannocaro, M. Rossi, A. Sacco, *Coord. Chem. Rev.* **1972**, *8*, 77; (b) M. Aresta, P. Giannocaro, M. Rossi, A. Sacco, *Inorg. Chim. Acta* **1971**, *5*, 115.

[12] J. M. Bellerby, M. J. Mays, P. L. Sears, *J. Chem. Soc., Dalton Trans.* **1976**, 1232.

[13] Gaussian 98, Revision A.7, M. J. Frisch, G. W. Trucks, H. B. Schlegel, G. E. Scuseria, M. A. Robb, J. R. Cheeseman, V. G. Zakrzewski, J. A. Montgomery, Jr., R. E. Stratmann, J. C. Burant, S. Dapprich, J. M. Millam, A. D. Daniels, K. N. Kudin, M. C. Strain, O. Farkas, J. Tomasi, V. Barone, M. Cossi, R. Cammi, B. Mennucci, C. Pomelli, C. Adamo, S. Clifford, J. Ochterski, G. A. Petersson, P. Y. Ayala, Q. Cui, K. Morokuma, D. K. Malick, A. D. Rabuck, K. Raghavachari, J. B. Foresman, J. Cioslowski, J. V. Ortiz, A. G. Baboul, B. B. Stefanov, G. Liu, A. Liashenko, P. Piskorz, I. Komaromi, R. Gomperts, R. L. Martin, D. J. Fox, T. Keith, M. A. Al-Laham, C. Y. Peng, A. Nanayakkara, C. Gonzalez, M. Challacombe, P. M. W. Gill, B. Johnson, W. Chen, M. W. Wong, J. L. Andres, C. Gonzalez, M. Head-Gordon, E. S. Replogle, and J. A. Pople, Gaussian, Inc., Pittsburgh PA, **1998**.

[14] P. Giannoccaro, A. Sacco, S. D. Ittel, M. A. Crushing, *Inorg. Synth.* **1977**, *17*, 69.